Journal of the Korean Physical Society, Vol. 73, No. 12, December 2018, pp. 1879∼1883

Analysis of Deep-Trap States in GaN/InGaN Ultraviolet Light-Emitting Diodes after Electrical Stress

Seonghoon Jeong and Hyunsoo Kim*
School of Semiconductor and Chemical Engineering, Semiconductor Physics Research Center, Chonbuk National University, Jeonju 54896, Korea

Sung-Nam Lee
Department of Nano-Optical Engineering, Korea Polytechnic University, Siheung 15073, Korea

(Received 28 June 2018, in final form 28 August 2018)

We analyzed the deep-trap states of GaN/InGaN ultraviolet light-emitting diodes (UV LEDs) before and after electrical stress. After electrical stress, the light output power dropped by 5.5%, and the forward leakage current was increased. The optical degradation mechanism could be explained based on the space-charge-limited conduction (SCLC) theory. Specifically, for the reference UV LED (before stress), two sets of deep-level states which were located 0.26 and 0.52 eV below the conduction band edge were present, one with a density of 2.41×10^{16} and the other with a density of 3.91×10^{16} cm^{-3}. However, after maximum electrical stress, three sets of deep-level states, with respective densities of 1.82×10^{16}, 2.32×10^{16} cm^{-3}, 5.31×10^{16} cm^{-3} were found to locate at 0.21, 0.24, and 0.50 eV below the conduction band. This finding shows that the SCLC theory is useful for understanding the degradation mechanism associated with defect generation in UV LEDs.

PACS numbers: 73.40.Kp, 73.40.Ns, 73.61.Ey
Keywords: Ultraviolet, Light-emitting diodes, Degradation, Deep-level states, Space-charge-limited conduction, Leakage current, Reliability
DOI: 10.3938/jkps.73.1879

I. INTRODUCTION

Recently, ultraviolet light-emitting diodes (UV LEDs) have been extensively investigated owing to their practical needs in a variety of fields depending on the UV wavelength [1–5]. For example, UV-A with an emission wavelength in the range of 315 - 400 nm is used for UV curing, counterfeit detection and printing, UV-B (280 - 315 nm) is used for medical and sensing applications, and UV-C (100 - 280 nm) is used for water/air disinfection, sensing and medical applications [3–5]. At present, the highest usage of UV LEDs is for curing applications, *i.e.*, UV-A, while UV-C has a much greater potential for applications in the disinfection of water and air. UV LEDs can be designed with an InGaN/GaN multiple- quantum-well (MQW) active region for UV-A, while AlGaN/GaN MQWs are required for shorter UV wavelengths (UV-B and C). In addition to its having highest penetration into market, the InGaN/GaN MQW structure can be relatively easily grown on a sapphire substrate by using metalorganic chemical deposition (MOCVD); therefore, high-efficiency or reliable UV LEDs with a UV-A wavelength are of particular importance.

UV LEDs, however, often suffer from poor reliability associated with epitaxial structural weakness and packaging issues [6–9]. For example, packaging materials such as encapsulants and materials with reflective surfaces can degrade under accelerated heating or UV irradiation [10–12]. With the advent of novel packaging materials and heat-dissipation design, however, this degradation mechanism seemed to be relatively insignificant [13]. Meanwhile, the most prevalent and unavoidable degradation mechanism in GaN-based UV LEDs is the formation of crystal defects in the active region, generating deep-level states at the MQWs and, hence, reducing the radiative recombination (or increasing the nonradiative recombination through the generated deep-level states) [6,7,14,15]. Therefore, understanding the generation of deep-level states during device operation is quite important for obtaining efficient, reliable UV LEDs.

The typical method for analyzing deep-level states is deep-level transient spectroscopy (DLTS). However, this method requires an expensive facility and elaborate sample preparation and measurement. On the one hand, recently, Nana *et al.* [16] reported a single-carrier space-charge-limited conduction (SCLC) theory to elucidate the origin of the excess forward leakage current of Al-

*E-mail: hskim7@jbnu.ac.kr

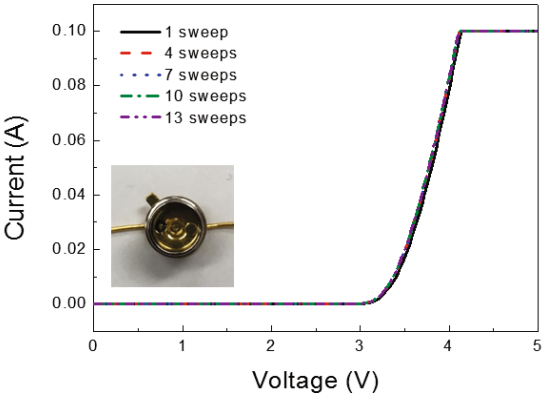

(a)

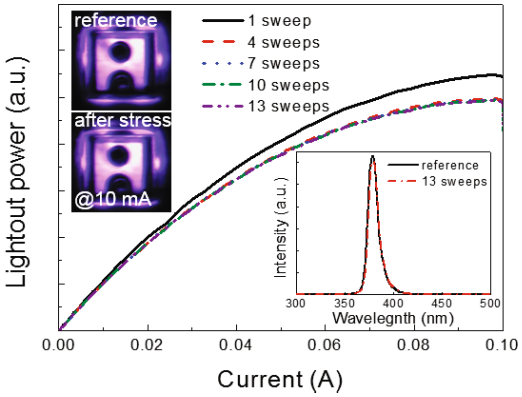

(b)

Fig. 1. (Color online) (a) I-V curves of UV LEDs for various numbers of I-V sweeps. A photographic image of UV LED is shown in the inset of Fig. 1(a). (b) The light output power versus current curves for various numbers of I-V sweeps. The inset shows the EL spectra and EL images taken at 10 mA for the reference and the stressed UV LEDs (13 sweeps).

GaN/InGaN double-heterostructure LEDs. Specifically, the density and the energy level of deep-trap states residing in the active region could be calculated according to SCLC model based on the power-law relationship in the low forward bias current-voltage (I-V) curves. Note that the SCLC model is more useful to explain the leakage current of LEDs at lower forward bias voltages or at larger reverse bias voltages as compared to the well-known hopping or Poole-Frenkel emission models [15]. Our group [17] also elucidated the presence of deep-level (or deep-trap) states in the GaN/InGaN MQW (emitting blue color) active region by using the SCLC theory. Indeed, this method is quite simple and does not require additional measurement facilities. In this study, we attempted to analyze commercial-grade UV LEDs based on SCLC theory. The UV LEDs were evaluated before and after electrical stress to further investigate the change of the deep-level states.

II. EXPERIMENTS

To prepare the UV LED lamp, we packaged a commercially available GaN/InGaN UV chip (purchased) onto a TO-10 stem. The peak emission wavelength of the UV chip was around 380 nm. After wiring, the chip was encapsulated with silicone resin (see the inset of Fig. 1(a)). The size of the UV chip was 300×300 μm^2 (see the inset of Fig. 1(b)). To investigate the I-V characteristics of the UV LEDs (lamp), we used a parameter analyzer (HP4156A). The light output power and the electroluminescence (EL) spectra were measured using a Si photodiode (883-UV) connected to the parameter analyzer and an optical spectrometer (Ocean Optics USB2000). The EL images were also obtained using a CCD camera attached to a probe station for an optical microscope. For the electrical stress, I-V sweeps of the UV LEDs in the forward bias range from 0 to 5 V with a maximum compliance current of 100 mA were repeatedly carried out; *i.e.*, the numbers of I-V sweep were 1 (reference), 4, 7, 10, and 13. For the electrical stress, the UV LEDs were placed onto the Cu chuck of the probe station; *i.e.*, the stress was performed at room temperature in an air ambient. After each I-V sweep, the forward I-V curve was analyzed based on SCLC theory.

III. RESULTS AND DISCUSSION

Figure 1(a) shows the I-V curves of UV LEDs for various numbers of sweeps. A photographic image of the UV LED is shown in the inset of Fig. 1(a). The UV LED is shown to have nominal operation with a forward voltage of 3.20 V at 20 mA. However, repeated I-V sweeps led to a very slight change in the forward I-V curves; *i.e.*, the forward voltage was reduced to 3.18 V after 13 sweeps. A reduced forward voltage after electrical stress or reliability testing, which is the so-called aging effect, has been frequently observed [18] and has been attributed to improved Ohmic contact to the p-GaN and/or dopant reactivation because substantial heat is generated during reliability or aging testing [19,20]. This implies that repeated I-V sweeps for aging testing results in a significant generation of heat. Considering that the UV chip was purchased and the I-V curve was quite nominal with low forward voltage (or low resistance), we were able to attribute the primarily origin of the I-V change after repeated sweeps to poor packaging; that is, the generated heat was not dissipated efficiently.

Indeed, significant Joule heating was seen in the light output power versus current plots (Fig. 1(b)), where the light output power has a sub-linear dependence on the current and even saturates at currents higher than 80 mA. In addition, the UV LED after repeated I-V sweeps showed a significant light output degradation; *i.e.*, the light output power dropped by 5.5% after $4 \sim 13$

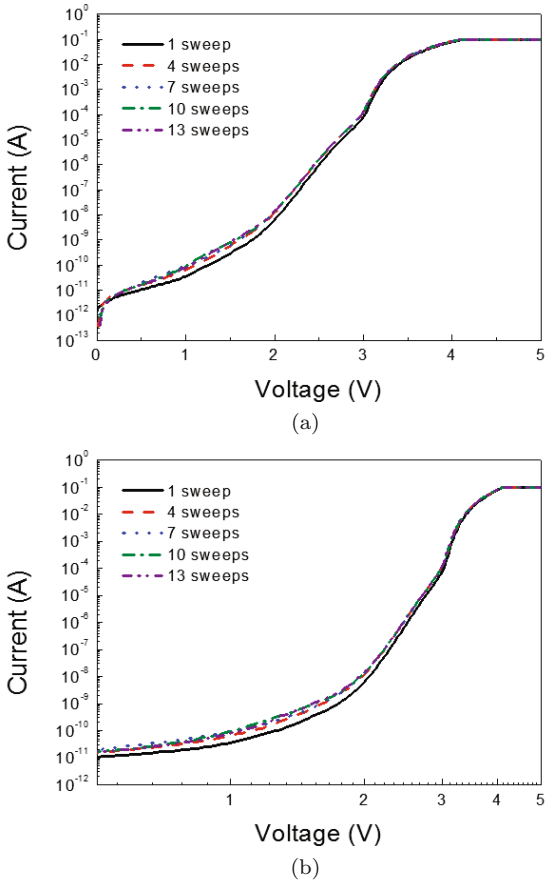

Fig. 2. (Color online) (a) Semi-logarithmic and (b) logarithmic I-V curves of UV LEDs for various numbers of I-V sweeps.

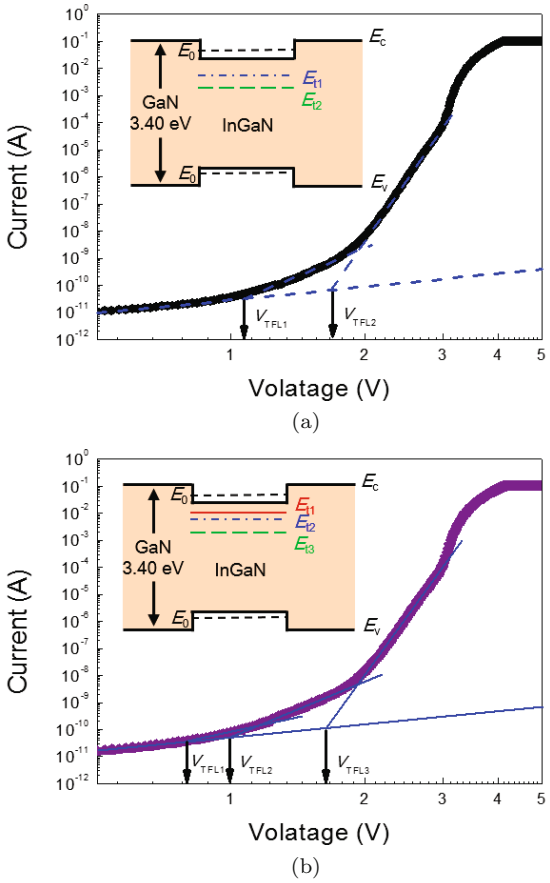

Fig. 3. (Color online) Semi-logarithmic I-V curves of the (a) reference UV LED and the (b) stressed UV LED (13 sweeps). The inset shows schematic band diagrams with deep-trap states.

I-V sweeps. Consistently, the EL spectra and the EL images obtained at 10 mA showed an output reduction after 13 I-V sweep, as shown in the inset of Fig. 1(b). If the output degradation is to be explained, first, the aging effect should be taken into consideration, According to the literature [6,7], however, the aging effect (favorable change in the forward voltage) has not been reported to have a negative influence on the output. Therefore, the output degradation after repeated I-V sweeps is hypothesized to have been solely due to Joule heating, which can accelerate the generation of deep-level states in the active region.

Our hypothesis was supported by the semi-logarithmically plotted I-V curves for various numbers of I-V sweeps, as shown in Fig. 2(a). For example, evidently, the forward leakage current in the low bias range ($V <\sim$3.0 V) was increased after repeated sweeps. This indicates that the number of deep-level states acting as a shunt path increases after electrical stress. However, in this low bias range, the carrier transport cannot be simply explained by using classical Shockley theory [21], *e.g.*, generation-recombination currents are dominant when $V <\sim$2.5 V and diffusion currents are dominant when $V >\sim$2.5 V, because a so-called hump is formed in the voltage range of $\sim$ 2 - 3 V [22]. Actually, this hump has very frequently been observed for the GaN-based LEDs and is responsible for the anomalously large ideality factors of $\sim$ 3 - 7 [23].

To further analyze the forward leakage current, we replotted the I-V curves logarithmically, as shown in Fig. 2(b). Evidently, the I-V curves have a power-law relationship [16,24,25], namely, $I \propto V^x$, where x is an exponent. This indicates that the forward leakage current can be understood in terms of SCLC theory, as reported previously [16, 17, 24, 25]. To use SCLC theory, similar to previous studies [26–28], we also applied the single-carrier injection model because, compared to electron traps, hole traps hardly occur at low biases. Originally, the SCLC theory was made to analyze the conduction in insulators having a large bandgap energy ($>$ 2.0 eV). Specifically, a very limited number of free carriers (n_0, generated by thermal excitation) dominates the overall conduction while the presence of a few deep-level states can modify the overall conduction by trapping the free carriers. Therefore, the trapping and subsequent full occupation of deep-level states can be clearly observed from

Table 1. All physical parameters of the reference and the stressed UV LED, as obtained from the V_{TFL} values and SCLC theory.

# of I-V sweep	V_{TFL} (V)	p_{t0} (cm^{-3})	n_0 (cm^{-3})	$E_{\mathrm{C}} - E_f$ (eV)
1	1.03	2.41×10^{16}	8.48×10^{13}	0.26
	1.67	3.91×10^{16}	3.80×10^{9}	0.52
4	0.88	2.06×10^{16}	4.04×10^{14}	0.22
	1.05	2.46×10^{16}	6.38×10^{13}	0.27
	1.66	3.88×10^{16}	7.36×10^{9}	0.50
7	0.85	1.99×10^{16}	6.70×10^{14}	0.21
	1.01	2.36×10^{16}	1.41×10^{14}	0.25
	1.63	3.81×10^{16}	9.92×10^{9}	0.50
10	0.8	1.87×10^{16}	6.79×10^{14}	0.21
	0.98	2.29×10^{16}	2.17×10^{14}	0.24
	1.64	3.84×10^{16}	1.08×10^{8}	0.61
13	0.78	1.82×10^{16}	5.98×10^{14}	0.21
	0.99	2.32×10^{16}	2.04×10^{14}	0.24
	1.64	5.31×10^{16}	1.17×10^{10}	0.50

the sharp changes in the slope of the logarithmic I-V curves, giving rise to x values larger than 2, as shown in Fig. 3. Therefore, by measuring the transition voltage (V_{TFL}) at which the slope changes sharply, one can calculate the density of deep-level states and their energy levels by using [16,17,24,25]

$$V_{\mathrm{TFL}} = \frac{q p_{t0} L^2}{\varepsilon \varepsilon_0} \tag{1}$$

$$\frac{J(2V_{\mathrm{TFL}})}{J(V_{\mathrm{TFL}})} \sim \frac{p_{t0}}{n_0} \tag{2}$$

$$n_0 = N_{\mathrm{C}} \exp\left[-\frac{(E_{\mathrm{C}} - E_f)}{kT}\right], \tag{3}$$

where p_{t0} is the concentration of the unoccupied traps (or deep-level states) in the QWs, L is the thickness of the active region (*i.e.*, the whole thickness of MQWs = 145 nm), ε is the relative dielectric constant (8.9), ε_0 is the permittivity of free space, J is the current density, N_{C} is the effective density of the states at a conduction band edge (2.3×10^{18} cm^{-3}), T is 298 K, and $E_{\mathrm{C}} - E_f$ is the energy distance between the conduction band edge (E_{C}) and the Fermi level (E_f).

In Fig. 3(a), the two V_{TFL} positions were observed as 1.03 and 1.67 V, which are in good agreement with the values for commercial-grade GaN/InGaN MQW blue LEDs [17]. This indicates that two predominant deep-level states are present in the reference UV LEDs, as shown in the inset of Fig. 3(a). However, after 13 I-V sweeps, as shown in Fig. 3(b), three V_{TFL} positions were observed at 0.78, 0.99 and 1.64 V, indicating that additional deep-trapping centers had been created. On the basis of Eqs. (1) - (3) and the obtained V_{TFL} values, the density of the deep-level states (p_{t0}) and the energy position of each deep-level states (corresponding to $E_{\mathrm{C}} - E_f$, where E_{C} is assumed to be equal to E_0 (the level of the ground states in QWs)) can be calculated; the results are summarized in Table 1. These results show that the electrical stress on the UV LEDs certainly led to the generation of additional deep-level states in the MQW active region (occurring as a result of Joule heating). The generated deep-level states are expected to accelerate nonradiative recombination and to suppress radiative recombination. Therefore, the output reduction of UV LED after electrical stress could be explained. Lastly, an investigation of the possible origins of the deep-level states would be meaningful. According to the literature, diffused Mg [29], dangling bonds [30], Mg-H-related defects [22], Ga vacancies [31,32], N vacancies [33,34], and structural defects such as dislocations [35] have been suggested as possible origins of the leakage currents. However, the precise mechanism is still being investigated.

IV. CONCLUSION

To summarize, the forward leakage current of GaN/InGaN UV LEDs was analyzed by using the SCLC model. After electrical stress, the UV LEDs showed a noticeable output drop accompanied by an evolution of a forward leakage current at low bias region. The anomalous forward I-V curve with a hump at around 2.5 V, however, could not be explained by using classical diode theory. This could be quantitatively analyzed based on SCLC model, *i.e.*, two sets of deep-level states with respective densities of 2.41×10^{16} and 3.91×10^{16} cm^{-3} at 0.26 and 0.52 eV below the E_{C} for the reference UV LEDs; on the other hand, the electrical stress generated one more set of deep-level states located at 0.21 eV below E_{C} with a density of 1.82×10^{16} cm^{-3}.

ACKNOWLEDGMENTS

This research was supported in part by the Basic Science Research Program through the National Research Foundation of Korea (NRF), funded by the Ministry of Education (2017R1A2B4007182) and in part by the Development of R&D Professionals on LED Convergence Lighting for Shipbuilding/Marine Plant and Marine Environments (Project No: N0001363) funded by the Ministry of Trade, Industry & Energy(MOTIE, Korea). This paper was also supported by the selection of a research-oriented professor of Chonbuk National University in 2018.

REFERENCES

[1] H. Hirayama, S. Fujikawa, N. Noguchi, J. Norimatsu, T. Takano, K. Tsubaki and N. Kamata, Phys. Stat. Sol. (a) **206**, 1176 (2009).

[2] U. Kasten, D. Beyersmann, J. Dahm-Daphi and A. Harwig, Mutat. Res. **336**, 143 (1995).

[3] H. Kudo, M. Sawai, Y. Suzuki, X. Wang, T. Gessei, D. Takahasho, T. Arakawa and K. Mitsubayashi, Sens. Actuator B-Chem. **147**, 676 (2010).

[4] J. Close, J. Ip and K. H. Lam, Renew. Energy **31**, 1657 (2006).

[5] J. L. Shie, C. H. Lee, C. S. Chiou, C. T. Chang, C. C. Chang and C. Y. Chang, J. Hazard. Mater. **155**, 164 (2008).

[6] M. Menegehini, L. R. Trevisanello, G. Meneghesso and E. Zanoni, IEEE Trans. Device Mater. Reliab. **8**, 323 (2008).

[7] M. Meneghini, A. Tazzoli, G. Mura, G. Meneghesso and E. Zanoni, IEEE Trans. Electron Dev. **57**, 108 (2010).

[8] M. A. Khan, Phys. Stat. Sol. (a) **203**, 1764 (2006).

[9] L. X. Zhao, E. J. Thrush, C. J. Humphreys and W. A. Phillips, J. Appl. Phys. **103**, 024501 (2008).

[10] E. Jung, M. Kim and H. Kim, IEEE Trans. Electron. Dev. **60**, 186 (2013).

[11] E. Jung, J. H. Ryou, C. H. Hong and H. Kim, J. Electrochem. Soc. **158**, H132 (2011).

[12] G. Meneghesso, S. Levada, R. Pierobon, F. Rampazzo, E. Zanoni, A. Cavallini, A. Castaldini, G. Scamarcio, S. Du and I. Eliasevich, in IEDM Tech. Dig. 103 (2002).

[13] R. Mueller-Mach, G. Mueller, M. Krames and T. Trottier, IEEE J. Sel. Top. Quantum Electron. **8**, 339 (2002).

[14] M. Meneghini, M. laGrassa, S. Vaccari, B. Galler, R. Zeisel, P. Drechsel, B. Hahn, G. Meneghesso and E. Zanoni, Appl. Phys. Lett. **104**, 113505 (2014).

[15] L. Hirsch and A. S. Barriere, J. Appl. Phys. **94**, 5014 (2003).

[16] R. Nana, P. Gnanachchelvi, M. A. Awaah, M. H. Gowda, A. M. Kamto, Y. Wang, M. Park and K. Das, Phys. Stat. Sol. (a) **207**, 1489 (2010).

[17] E. Jung, S. Jeong, J. H. Ryou and H. Kim, J. Nanosci. Nanotechnol. **17**, 7339 (2017).

[18] L. R. Trevisanello, M. Meneghini, G. Mura, C. Sanna, S. Buso, G. Spiazzi, M. Vanzi, G. Meneghesso and E. Zanoni, Proc. SPIE **6669**, 666913 (2007).

[19] L. Trevisanello, M. Meneghini, G. Mura, M. Vanzi, M. Pavesi, G. Meneghesso and E. Zanoni, IEEE Trans. Device Mater. Reliab. **8**, 304 (2008).

[20] M. Meneghesso and E. Zanoni, IEEE Trans. Electron Dev. **53**, 2981 (2006).

[21] W. Shockley and Bell Syst. Tech. J. **28**, 435 (1949).

[22] H. Kim, J. Cho, Y. Park and T. Y. Seong, Appl. Phys. Lett. **92**, 092115 (2008).

[23] D. Zhu, A. N. Noemaun, J. Kim, E. F. Schubert, M. H. Crawford and D. D. Koleske, Appl. Phys. Lett. **94**, 081113 (2009).

[24] M. A. Lambert and P. Mark, *Current Injection in Solids* (Academic Press, New York, 1970).

[25] A. Rose, Phys. Rev. **97**, 1538 (1955).

[26] J. Osaka, Y. Ohno, S. Kishimoto, K. Maezawa and T. Mizutani, Appl. Phys. Lett. **87**, 222112 (2005).

[27] A. Hierro, S. A. Ringel, M. Hansen, J. S. Speck, U. K. Mishra and S. P. Denbaars, Appl. Phys. Lett. **77**, 1499 (2000).

[28] T. Mattila and R. M. Nieminen, Phys. Rev. B **54**, 16676 (1996).

[29] A. Mao, J. Cho, Q. Dai, E. F. Schubert, J. K. Son and Y. Park, Appl. Phys. Lett. **98**, 023503 (2011).

[30] V. Kuksenkov, H. Temkin, A. Osinsky, R. Gaska and M. A. Khan, Appl. Phys. Lett. **72**, 1365 (1998).

[31] J. Toivonen, T. Hakkarainen, M. Sopanen, H. Lipsanen, J. Oila and K. Saarinen, Appl. Phys. Lett. **82**, 40 (2003).

[32] R. Armitage, W. Hong, Q. Yang, H. Feick, J. Gebauer, E. R. Weber, S. Hautakangas and K. Saarinen, Appl. Phys. Lett. **82**, 3457 (2003).

[33] M. W. Bayerl, M. S. Brandt, O. Ambacher, M. Stutzmann, E. R. Glaser, R. L. Henry, A. E. Wickenden, D. D. Koleske, T. Suski, I. Grzegory and S. Porewski, Phys. Rev. B **63**, 125203 (2001).

[34] Q. Yan, A. Janotti, M. Scheffler and C. G. van de Walle, Appl. Phys. Lett. **100**, 142110 (2012).

[35] L. Lymperakis, J. Neugebauer, M. Albrecht, T. Remmele and H. P. Strunk, Phys. Rev. Lett. **93**, 196401 (2004).